Crystal and local structure changes in Janh-Teller systems of Cu(II) and Mn(III) induced by pressure. Study of the dissappearance of the AFD structure.

Fernando RODRÍGUEZ*, Fernando AGUADO, Jean-Paul ITIÉ[1] and Michel HANFLAND[2]

DCITIMAC, Facultad de Ciencias, Universidad de Cantabria, Santander 39005, Spain
[1]*Université Pierre et Marie Curie, B77 4 Place Jussieu 75252 Paris Cedex 05, France*
[2]*ESRF, BP 220, 38043 Grenoble, France*

This work investigates the variation of local structure around Cu^{2+} and Mn^{3+} as a function of pressure in A_2CuCl_4 and $AMnF_4$ layered perovskites by means of x-ray absorption, optical spectroscopy and x-ray diffraction. In both families pressure induces simultaneously reduction of the Jahn-Teller distortion (JTD) and tilting of the $CuCl_6^{4-}$ and MnF_6^{3-} octahedra. The JTD release is attained by decreasing both the equatorial and axial Cu-Cl and Mn-F bond distances with pressure, ΔR_{ax} being almost an order magnitude bigger than ΔR_{eq}. We show that the JTD is stable in a wide pressure range. Estimates based on structural data and JT energy indicate that JT suppression would occur above 20 GPa.

1. Introduction

The A_2CuCl_4 (A=Rb,$C_nH_{2n+1}NH_3$; n=1-3) [1-9] and $AMnF_4$ (A: Rb, Na, Tl, Cs) [10-16] layered compounds present a large variety of interesting physical phenomena associated with antiferrodistortive (AFD) structure displayed by the Jahn-Teller (JT) axially elongated $CuCl_6^{4-}$ and MnF_6^{3-} complexes, respectively. They have attracted interest as two-dimensional ferromagnets with $T_c \approx 10$ K [1,3,7,8,10,11], as related material to high T_C superconductors and colossal magnetoresistors [17], as an organic/inorganic hybrid layered system, and as piezochromic materials [5,13]. In the last years an intense activity aimed to investigate the behavior of these materials under hydrostatic pressure, in particular, for exploring pressure-induced structural transitions associated with the disappearance of the AFD structure and tilting phenomena [3-8,14]. The former effect is noteworthy since it must lead to a switch in the 2D magnetic behavior from ferromagnetic to antiferromagnetic.

Recent structural studies devoted to determine the possible disappearance of the JTD by pressure reported controversial results in both Cu^{2+} and Mn^{3+}. Firstly, structural studies by x-ray diffraction (XRD) and x-ray absorption (XAS) in $(C_3H_7NH_3)_2CuCl_4$ [7] and $(C_2H_5NH_3)_2CuCl_4$ [8,9] concluded, in the latter case, that the JTD is suppressed at 4 GPa ($R_{ax} \approx R_{eq}$) in agreement with Raman data [8]. However, correlation studies between lattice parameters from XRD and Cu-Cl bond distances from EXAFS in $(C_3H_7NH_3)_2CuCl_4$ [7] showed that although the reduction of the Cu-Cl axial distance with pressure, ΔR_{ax}, is longer than ΔR_{eq}, in no way the JTD is suppressed below 10 GPa. A similar situation occurred for $LaMnO_3$ [18,19]. Neutron diffraction under pressure indicates that the MnO_6 JTD is stable in the 0-6 GPa range [18], whereas XRD reveals that pressure gradually reduces the JTD yielding suppression at about 10 GPa [19]. This controversy is likely due to difficulties to perform precise analysis of the diffracted intensity, providing the M-X bond distances of the MX_6 polyhedra. In general, the M-X distances and their variation with pressure in perovskites can be difficult in cases where the structural information can not be derived from the cell parameters but from intensity analysis. The problem is even harder if as in the present case we deal with AFD structures. XRD powder diagrams often exhibit intensity deviations due to preferential orientation, twining, texture and dynamical JT effects that can hinder analysis of the diffracted intensity associated with JTD. The use of local probes like EXAFS [7] or optical absorption (OA) spectroscopy [13-16] is crucial for an appropriate local structural determination. XAS studies on $LaMnO_3$ [20] and OA in $NaMnF_4$ [4] are examples illustrating the usefulness of local probes to detect structural effects unrevealed by XRD.

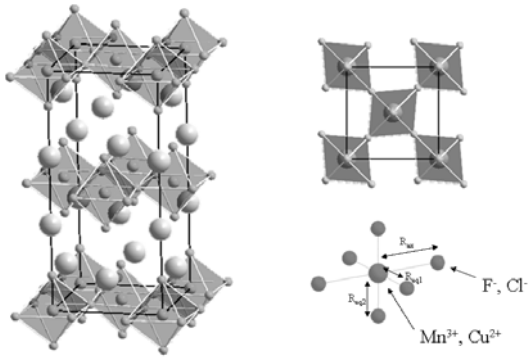

Fig. 1. Crystal structure of layered perovskites $AMnF_4$, showing the antiferrodistortive structure displayed by the MnF_6^{4-} complexes, whose local structure is sketched bottom right. A similar layered structure of interconnected $CuCl_6^{4-}$ units is found for A_2CuCl_4.

The present work deals with structural correlation studies in JT systems of Cu^{2+} and Mn^{3+} carried out in crystal series and as a function of pressure. The aim is to explore the structural variation of crystal and around the JT ion in the layer perovskites A_2CuCl_4 and $AMnF_4$ and how they influence materials properties. The knowledge of whether pressure reduces the JTD or induces tilts is necessary to understand and, eventually predict, magnetic, electrical and optical properties in these compounds. We present structural studies on layer-perovskite series carried out by XRD, XAS and OA spectroscopy. In Mn^{3+} fluorides, we show that OA is a suitable technique for establishing correlations between the optical spectra and the local structure around Mn^{3+}. Besides, optical spectroscopy provides information on the electron-ion coupling, JT energy and exchange interaction between JT ions [15]. Interestingly, we use OA to investigate

variations of local structure around Mn^{3+} and elucidate whether pressure can yield structural changes associated with the high-spin to low-spin ground-state transition. We present investigations of this structural effect in $CsMnF_4$.

2. Experimental

Single crystals of $(CH_3NH_3)_2CuCl_4$ and $CsMnF_4$ examined in pressure experiments, were grown from solution as described elsewhere [2,16]. The OA experiments under pressure were done using the experimental setups for using high-pressure techniques reported elsewhere [15]. XRD under pressure in $CsMnF_4$. was performed in the ID09 white beam station at the European Synchrotron Radiation Facility (ESRF) in Grenoble. Experiments were done on a membrane diamond anvil cell (DAC) at room temperature using helium as pressure transmitter. X-ray powder diffractograms were obtained as a function of pressure in the 0-16 GPa range using wavelength, λ = 0.4124 Å, which is far enough from the spectral region of the diamond absorption. XAS experiments under pressure in $(CH_3NH_3)_2CuCl_4$ have been performed at the absorption setup XAS10 of the D11 beamline at LURE (Orsay). The XAS spectra were measured at the Cu k-edge (E_0 = 8.98 keV) at room temperature using dispersive EXAFS in the 8.9-9.3 keV range. This experimental setup has been proved to be very sensitive for obtaining suitable EXAFS oscillations in a wavelength range where the diamond anvil absorption is very strong. D11 provides adequate beam coherence and intensity to do suitable EXAFS under pressure [21]. The incident beam intensity at the sample within the hydrostatic cavity was about 10^{10} photons/mm^{2}sec. In order to avoid radiation damage, each spectrum was taken in about 15 sec. Different loading cycles were done for each compound. The pressure was applied with a membrane-type DAC employing paraffin oil as pressure transmitter. The squeezed powder became opaque (black) at 10 GPa according to the pressure-induced band-gap redshift, but transparency was recovered upon pressure release. EXAFS spectra were analysed on the basis of a $CuCl_6^{4-}$ unit with three different Cu-Cl distances: R_{eq1}, R_{eq2} and R_{ax}. In all pressure experiments, the pressure was measured from the R-line shift of Ruby chips introduced in the hydrostatic cavity.

3. Results and discussion

3.1 XAS experiments under pressure in $(CH_3NH_3)_2CuCl_4$

Table 1 reports structural data corresponding to the A_2CuCl_4 series at room temperature. It is worthnoting that the JTD, represented through the normal coordinate, $Q_\theta = \sqrt{\frac{4}{3}}(R_{ax} - R_{eq})$, reduces with the cell volume from 0.87 to 0.51 Å on passing from $(C_3H_7NH_3)_2CuCl_4$ (V = 1400 Å^3) to Rb_2CuCl_4 (800 Å^3), respectively. This large volume change is, however, mainly governed by the size of the alkyl-ammonium ion, since the corresponding in-layer Cu-Cu distance varies from 5.30 to 5.05 Å. It means that layers to a great extent maintain its characteristic structure along the series at ambient pressure. Nevertheless, it does not occur in pressure experiments because the layer compressibility is similar to compressibility along **c** in spite

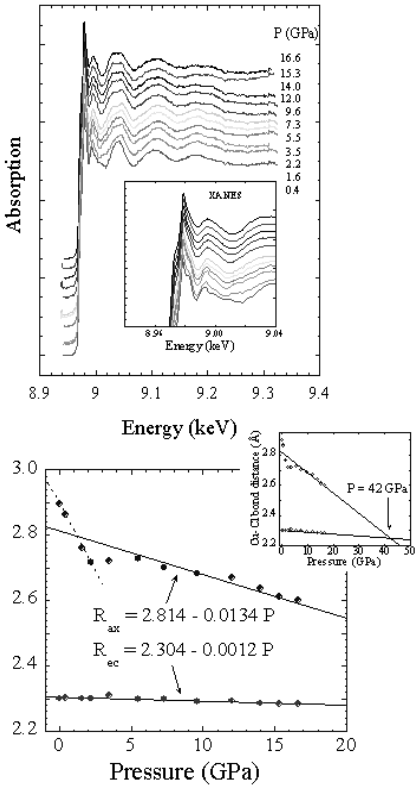

Fig. 2. (Top) XAS spectra of $(CH_5NH_3)_2CuCl_4$ powders as a function of pressure. The inset shows a magnification of XANES. (Bottom) Variation of the Cu-Cl bond distances, R_{eq} and R_{ax}, deived from EXAFS with pressure. The lines and associated equations correspond to least-square fit. The inset shows extrapolated data for JT suppression ($R_{eq} = R_{ax}$).

of the large anisotropy exhibited by these layered compounds. XRD pressure experiments carried out in $(C_3H_7NH_3)_2CuCl_4$ and $(C_2H_5NH_3)_2CuCl_4$ show that the relative variation of the Cu-Cu distance, R_{Cu-Cu}, and c is similar. In particular, the cell volume reduces from 1400 to 1000 Å^3 (78%) in $(C_3H_7NH_3)_2CuCl_4$ [1170 to 910 Å^3 (71%) in $(C_2H_5NH_3)_2CuCl_4$] in the 0 – 6 GPa range. Likewise, R_{Cu-Cu} and c vary from 5.3 to 4.9 Å (92%) [5.2 to 4.8 Å (91%)] and from 24 to 22 Å (92%) [21.2 to 20.0 Å (94%)], respectively, in the same range. Note that $(C_3H_7NH_3)_2CuCl_4$ is more compressible and isotropic than $(C_2H_5NH_3)_2CuCl_4$. However, the variation of $R_{ax} + R_{eq}$, derived from EXAFS, is different from the R_{Cu-Cu} variation. Whereas R_{Cu-Cu} reduces -0.4 Å from 0 to 6 GPa, $R_{ax}+R_{eq}$ decreases -0.2 Å, in both $(C_3H_7NH_3)_2CuCl_4$ [7] and $(CH_3NH_3)_2CuCl_4$ (Fig. 2). The distinct behavior must be ascribed to pressure-induced $CuCl_6^{4-}$ tilting. The rapid decrease of R_{ax} between 0 and 2 GPa, compared to the slight variation above 2 GPa, and the changes in the XANES spectra (inset of Fig. 2) likely indicates the occurrence of a pressure-induced phase transition at 2 GPa in $(CH_3NH_3)_2CuCl_4$. However, it deserves confirmation by XRD. Nevertheless no trace of structural phase transition has been observed in $(C_3H_7NH_3)_2CuCl_4$ from XRD and XAS, although the Cu-Cl distance variations with pressure are similar in both compounds. A salient conclusion is the different compressibility of the bulk and the $CuCl_6^{4-}$ octahedron, being about an order of magnitude smaller in the latter [7]. This behavior explains why JT suppression has not been

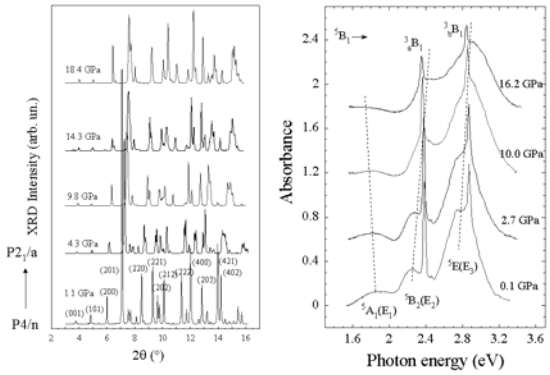

Fig. 3. (Left) XRD as a function of pressure in $CsMnF_4$. A tetragonal to monoclinic phase transition takes place at 2 GPa. (Right) Variation of the corresponding OA spectrum in the 0–16 GPa range. Peak labels correspond to axially elongated D_4 symmetry for MnF_6^{4-}. The lines are eye guides to illustrate pressure shifts of the JT-related three-band structure. Note the decrease of narrow peak intensity with pressure.

observed below 10 GPa in these two layered compounds Linear extrapolation of R_{ax} and R_{eq} indicates that JT suppression, $R_{ax} \approx R_{eq}$, would be attained above 20 GPa. This result contrasts to findings in $(C_2H_5NH_3)_2CuCl_4$ from XRD [9], where JT suppression takes place at the orthorhombic-to-monoclinic structural phase transition at 4 GPa. Interestingly, the energy of the a_{1g} $(3z^2)$ $\rightarrow b_{1g}$ $(x^2\text{-}y^2)$ transition (E_1= 1 eV) derived from crystal-field spectroscopy in A_2CuCl_4 [2], which is to the JT energy by $E_1 = 4\ E_{JT}$, indicates that the free-energy associated with the JTD is about 0.25 eV. Simple estimates based on the local compressibility of $CuCl_6^{4-}$ point out that the pressure required to transform an axially elongated coordination to a nearly octahedron would be roughly $P \approx E_{JT}/\Delta V > 20$ GPa. The local bulk modulus derived from EXAFS in $(C_3H_7NH_3)_2CuCl_4$ [7] is in agreement with present estimates.

This result together with the structural studies carried out in layered perovskites of Mn^{3+} support this view.

3.2 XRD and OA under pressure in $CsMnF_4$

The study of Mn^{3+} $(3d^4)$ in layered structures illustrates the usefulness of spectroscopy to obtain information on the local structure and the JT effect. Like A_2CuCl_4, Mn^{3+} in fluorides exhibits an axially elongated octahedron due to the JT effect [10-16]. In $CsMnF_4$ layer ferromagnet, the Mn-F bond distances are R_{ax}= 2.17 Å and R_{eq}= 1.84 Å (Q_θ= 0.38 Å; Q_ε= 0.04 Å) at ambient conditions. The structural characterization of Mn^{3+} systems and their behaviour under high pressure have been the object of intense investigations with some controversial results [18,19]. The AFD structure of Mn^{3+} in $AMnF_4$ (A: Na, Tl, Cs) makes difficult local structure determination around Mn^{3+} from XRD. Furthermore XAS at the Mn k-edge is very limited on dealing with DAC due to the strong absorption of diamonds around 7 keV. Nevertheless, OA spectroscopy under pressure provides a direct way of measuring the variation with pressure of the JT energy as well as the corresponding electron-lattice coupling parameters [15].

Figure 3 shows the variations of XRD and OA spectrum of $CsMnF_4$ as a function of pressure. Like $NaMnF_4$ [14], the spectrum consists of three broadbands, E_1 =1.89 eV, E_2 =2.24 eV and E_3 =2.79 eV, corresponding to vibronically-induced electric-dipole (ED) transitions within d^4 from the $^5B_1$ ground state to the $^5A_1$, $^5B_2$ and ^5E excited states, respectively. The structure reflects the d-splitting pattern due to the D_4 JT distortion of MnF_6^{3-}. E_1, E_2 and E_3 provide the so-called equatorial CF, 10Dq(eq) = E_2, and the tetragonal splitting of the parent O_h e and t_2 orbitals, $\Delta_e = E_1 = 4E_{JT}$, and $\Delta_t = E_3 - E_2$. According to established correlations [15], 10Dq(eq) depends on the equatorial Mn-F distance, R_{eq}, whereas Δ_e and Δ_t vary linearly with the tetragonal and rhombic normal coordinates, Q_θ and Q_ε, through the electron-ion E⊗e and T⊗e coupling coefficients, respectively [15],

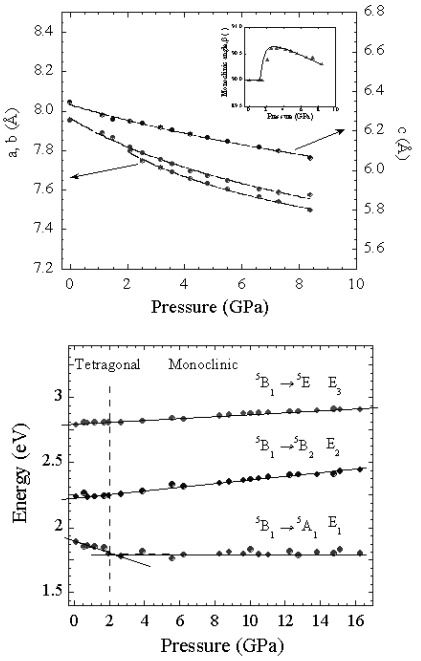

Fig. 4. (Top) Variation of the cell parameters *a*, *b*, *c* and *β* with pressure derived from XRD data of Fig. 3. (Bottom) Variation of E_1, E_2 and E_3 with pressure in $CsMnF_4$. The lines correspond to least-square fits. The slopes are -0.4 (0-2 GPa) and +0.2 (2-16 GPa) meV/GPa for E_1, and 14 and 9 meV/GPa for E_2 and E_3, respectively, in the 0-16 GPa range: Δ_t = 550 - 5 P (meV/GPa).

Table I. Variation of the local structure of MnF_6^{4-} with pressure in $CsMnF_4$. The Mn-F bond distances were obtained from E_1, E_2 and E_3 (Fig.4) following procedure established elsewhere [15]. The phase transition at 2 GPa involves rhombic distortions around Mn^{3+} (see text).

Crystal structure	Tetragonal *P4/n*		Monoclinic *P2₁/a*
R, Q (Å)	0 GPa	2 GPa	10 GPa
R_{ax}	2.17	2.15	2.04
R_{eq1}	1.82		1.92
R_{eq2}	1.85		1.71
R_{eq}	1.84	1.83	1.81
Q_θ	0.38	0.36	0.27
Q_ε	0.04	0.04	0.20

$$\Delta_e = 5.1\ Q_\theta \qquad \Delta_t = 1.4\ Q_\theta \qquad \text{(eV, Å)} \qquad (1)$$

The narrow peaks, E_{SP1} =2.39 eV and E_{SP2} =2.88 eV, correspond to spin-flip transitions $^5B_1 \rightarrow {}^3B_1$ in D_{4h}, whose ED mechanism is activated by exchange [13,14]. Their intensity decreases with MnF_6^{4-} tilting, i.e. deviations of the

in-layer Mn-F-Mn bond angle from 180º. Therefore, its intensity can be used as probe for tilting phenomena in pressure experiments. On the other hand, we can derive the variation of local structure with pressure from E_1, E_2 and E_3 provided that we know the pressure dependence of the linear electron-phonon coupling with the local modes a_{1g} and e_g, and the fact that the $^5B_1 \rightarrow {}^5B_2$ transition energy depends on R_{eq}, as [14-16] :

$$E(^5B_{2g}) = \frac{K}{R_{eq}^5} \qquad (2)$$

Following the procedure established elsewhere[14], we have determined the variations of the crystal and local structures in $CsMnF_4$ as a function of pressure using both the XRD and OA data in the 0 -16 GPa range (Fig. 4 and Table I).

As regards the variation of the OA spectrum of $CsMnF_4$ with pressure we conclude that JTD is stable in the explored pressure range. Pressure-induced suppression of JTD yielding a nearly O_h coordination must be ruled out since it would lead to an OA spectrum consisting of one broad band associated with the $^5E \rightarrow {}^5T_2$ transition. The observation of three broad bands confirms the JTD stability. Furthermore, the spin-flip peak intensity decreases with pressure, thus indicating pressure-induced MnF_6^{4-} tilts. This noteworthy result reflects the similarity of volume reduction effects upon tilting whatever induced by hydrostatic pressure or along the $AMnF_4$ crystal series. It must be noted that the in-layer Mn-Mn distance varies from 5.63 to 5.31 Å in the 0-10 GPa range. Such variation is similar to the Mn-F distance difference, $R_{ax} - R_{eq} = 0.33$ Å, attained in $CsMnF_4$ at ambient pressure, thus indicating that the JTD would disappear at 10GPa ($R_{ax} \approx R_{eq}$; $Q_\theta \approx 0$) provided that no tilting occurs. The OA spectrum clearly shows the existence of JTD up to 16 GPa, and consequently pressure-induced tilts must be invoked to maintain the MnF_6^{4-} JTD. The pressure behaviour of spin-flip peaks supports this view.

The linear variation of the JT splitting, $\Delta_e = E_1$, with pressure is different below and above 2 GPa. The slope, $\frac{d\Delta_e}{dP}$, changes from -4.2 meV/GPa in the 0 - 2 GPa range to +0.2 meV/GPa in the 2 -14 GPa range. The slope jump is related to the tetragonal-to-monoclinic structural phase transition, which takes place in $CsMnF_4$ at 2 GPa. The splitting of the (022) Bragg peak above 2 GPa in XRD confirms the monoclinic high-pressure phase in $CsMnF_4$ (Fig. 3). It is worth noting that the slope change of Δ_e is not observed for Δ_t. Given that Δ_t and Δ_e depends on Q_θ and $(Q_\theta^2 + Q_\varepsilon^2)^{1/2}$, respectively, the phase transition should involve mainly a rhombic distortion in the JTD MnF_6^{4-}. Table I shows the local structure variation of MnF_6^{4-} obtained from the pressure band shifts and cell parameter variations. Extrapolations suggest that the JTD would be suppressed at about 50 GPa. A structural phase transition associated with the simultaneous suppression of the JTD and high spin to low spin transition has been observed at 37 GPa.

4. Conclusion

The observed structural variations confirm the instability of the AFD layered structures under pressure in A_2CuCl_4 and $AMnF_4$. However, pressure induces both a reduction of the JTD and tilts of the $CuCl_6^{4-}$ and MnF_6^{3-} octahedra. The JTD is stable in the 0 - 10 GPa range, but can be eventually suppressed above 20 GPa according to the JT energy of Cu and Mn in their respective layered compounds. Interestingly, tilts preserve the axially elongated JTD in a wide pressure range, thus reflecting the strong molecular character of the JT complex.

Acknowledgment

This work was financed by the Spanish MEyC (Project Ref. MAT2005-00099). F.R. acknowledges partial support from the I3 Research Program of the University of Cantabria. XAS and XRD experiments were done at D11/LURE under proposal (Project PS 048-03), and ID09A/ESRF (Project HS 2159), respectively.

1) L.J. de Jongh and , A.R. Miedema, Advan. Phys. **23** (1974) 1.
2) R. Valiente and F. Rodríguez, J. Phys. Chem. Solids **57** (1996) 571.
3) T. Sekine, T. Okuno and K. Awaga, Chem. Phys. Lett. **249** (1996) 201.
4) Y. Moritomo and Y. Tokura, J. Chem. Phys. **101** (1994) 1763.
5) R. Valiente and F. Rodríguez, Phys. Rev. B **60** (1999) 9423.
6) M.A. Hitchman, Comments Inorg. Chem. **15** (1994) 197.
7) F. Rodríguez., M. Hanfland, J.P. Itié, and A. Polian: *Frontiers of high pressure research II. Application of high pressure to low-dimensional novel electronic materials* edited by Hochheimer, Kuchta, Dorthout and Yarger, (Kluwer Academic Publishers, Dordrecht 2001) Vol.48 pg. 143
8) F. Aguado, F. Rodríguez, R. Valiente and A. Señas, J.Phys. Cond. Matter, **16** (2004) 1927.
9) K. Ohwada et al., Phys. Rev. B **72** (2005) 014123.
10) F. Palacio and M.C. Morón: *Research Frontiers in Magnetochemistry* (World Scientific, 1992).
11) M.C. Moron, F. Palacio, S.M. Clark, and A. Paduan-Filho, Phys. Rev. B **51** (1995) 8660; Phys. Rev. B **54** (1996) 7052.
12) D. Oelkrug, Struct. Bond. 9, 1 (1971).
13) F. Rodríguez, P. Núñez, and C. Marco de Lucas, J. Solid State Chem. **110** (1994) 370.
14) F. Aguado, F. Rodríguez, and P. Núñez, Phys. Rev. B **67** (2003) 205101.
15) F. Rodríguez and F. Aguado, J. Chem. Phys.**118** (2003) 10867.
16) F. Aguado*: Ph.D. Thesis* (University of Cantabria, 2005).
17) J.M. De Teresa et al., Phys. Rev. B **65** (2002) 100403.
18) L. Pinsard-Gaudart, et al. Phys. Rev. B **64** (2001) 064426.
19) I. Loa, et al., Phys. Rev. Lett. **87** (2001) 125501.
20) M. C. Sánchez, G. Subías, J. García, and J. Blasco Phys. Rev. Lett. **90** (2003) 045503.
21) A. Sadoc et al., Phil. Mag. B **70** (1994) 855.